Supporting Information for:

Specific and Non-Specific Interactions of Fibronectin with Zwitterionic Peptoid Brushes Studied by Molecular Dynamics Simulation

David L. Cheung,[1,*] Phillip B. Messersmith,[2,3,4] King Hang Aaron Lau[5,*]

[1] *School of Biological and Chemical Sciences, University of Galway, Galway, Ireland;*

[2] *Department of Bioengineering, University of California, Berkeley, USA;*

[3] *Department of Materials Science and Engineering, University of California, Berkeley, CA 94720, USA;*

[4] *Materials Sciences Division, Lawrence Berkeley National Laboratory, Berkeley, CA 94720, USA;*

[5] *Department of Pure and Applied Chemistry, University of Strathclyde, Glasgow, UK;*

*Corresponding authors: david.cheung@universityofgalway.ie, aaron.lau@strathclyde.ac.uk

1. Supplementary Figures and Tables

1.1. Protein adsorption and brush preparation thickness data

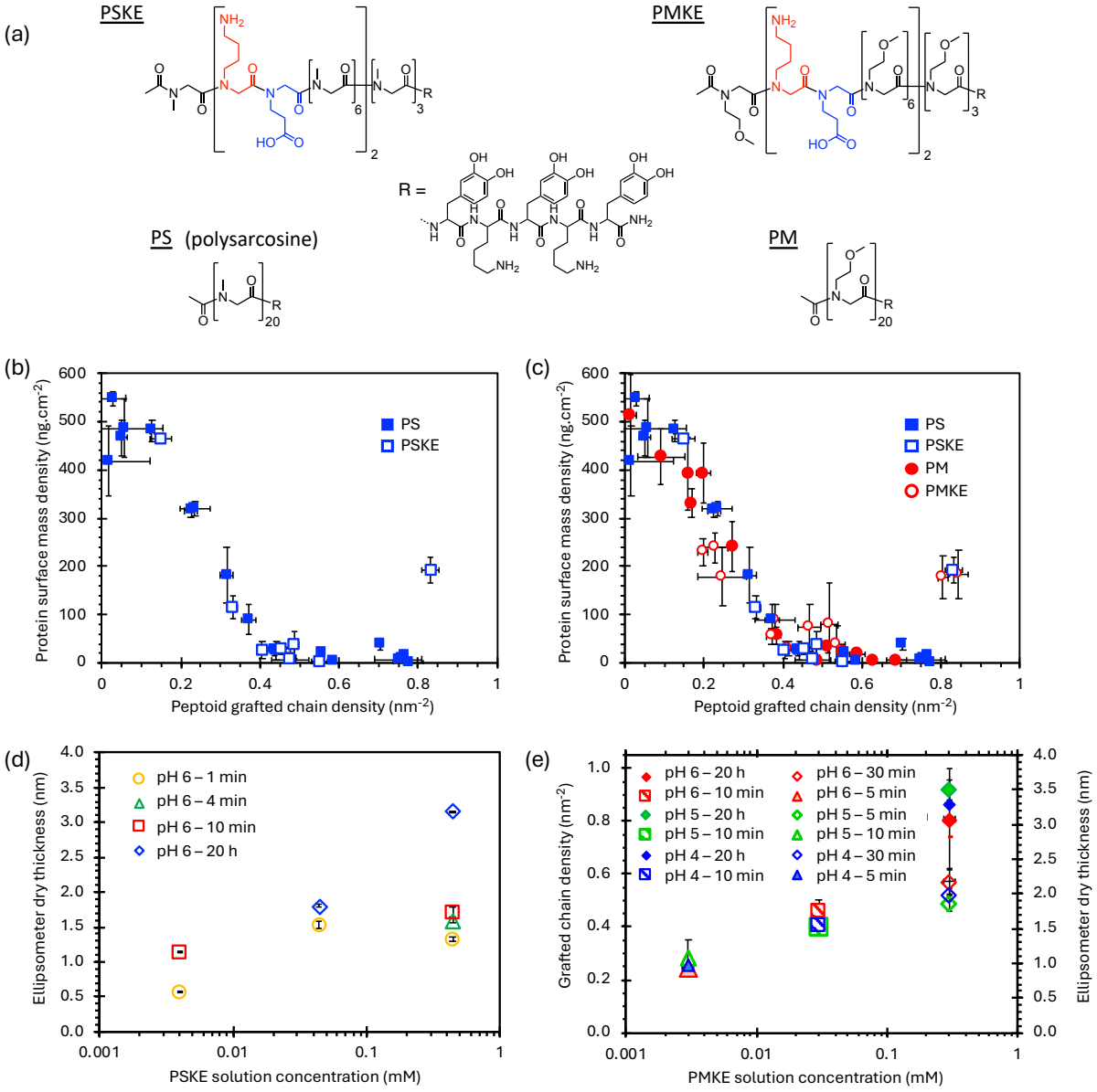

Fig.S1 (a) Chemical structures of PSKE, PS, PMKE and PM. (b) Copy of Fig.1c, for reference, showing protein adsorption on PSKE and PS peptoid brushes grafted over a range of surface chain densities. Data for PS is from reference 12 in the main text. All data refer to 20-mer peptoid chains. (c) Data in Fig.1c plotted together with protein adsorption data for PMKE and PM brushes. Data for PM is from reference 15. Data for PMKE is a combination of new data and data previously published in reference 15. All data refer to 20-mer peptoid chains. (d) The PSKE peptoid layer dry thickness measured by ellipsometry plotted against the solution concentration and incubation time used for deposition. Estimates of the grafted chain densities follow the left-y-axis plotted for PMKE chains shown (e), which plots the dry layer thickness for new PMKE layers prepared also using various solution conditions and incubation times for deposition. For both PSKE and PMKE layers, the calculation of chain density from dry layer thickness was established in the aforementioned publications (ref. 12,, 15) and it is possible because their chain molecular weights and volumetric densities are known for these monodisperse peptoid sequences.

1.2. Water Density Profiles

Water density profiles for the different surfaces are presented in Fig.S2. These are similar to those reported previously (Langmuir, 35, 1483), with pronounced layering near the surface of the rutile slab, a region of depleted (but not zero) density within the brush, and then a constant region with density approximately equal to bulk water outside the brush. The size of the depleted region and the decrease in density is greater for the Nchain=60 brushes compared to the Nchain=12 brushes. The water density far from the brush surface has been calculated for each system (Table S1) and is similar to that of bulk water in all cases (see Table S1).

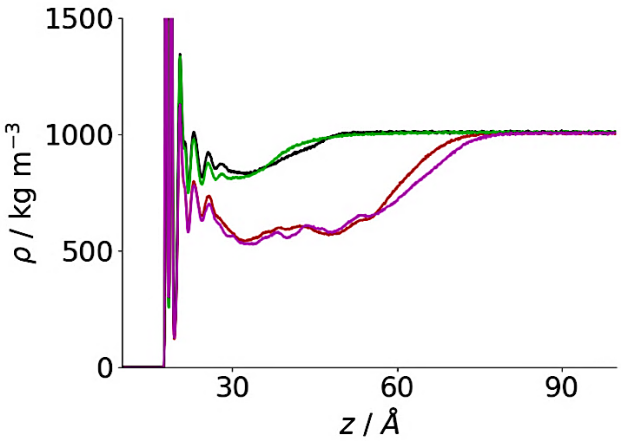

Fig.S2 Water density profiles for PS20 Nchain12 (black), PS20 Nchain60 (red), PSKE20 Nchain12 (green), PSKE20 Nchain60 (magenta).

Table S1. Calculated bulk water densities

	Bulk water density / kg m^{-3}
PS20 Nchain12	998.6±10
PS20 Nchain60	995.5±10
PSKE20 Nchain12	998.2±10
PSKE20 Nchain60	995.2±10

1.3. Adsorption free energies calculated for each simulation run

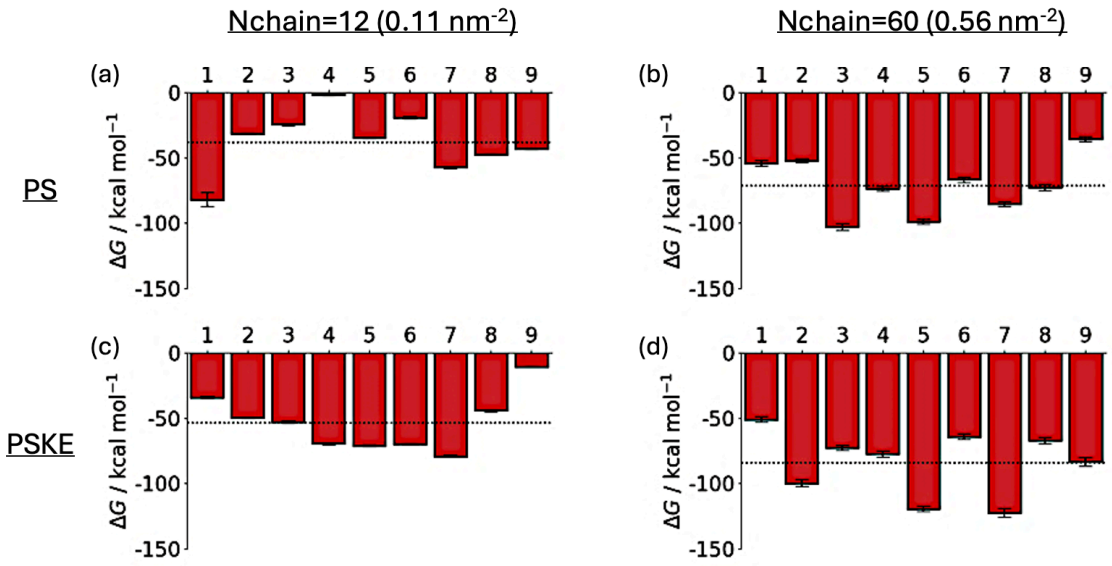

Fig.S3 Average adsorption free energies for each simulation run (averaged over the last 50 ns) for (top to bottom) $FnIII_{9-10}$ on PS Nchain=12, PS Nchain=60, PSKE Nchain=12, and PSKE Nchain=60. Dotted line shows average across all runs.

MM-PBSA calculations showed that, as expected, the total interaction was more attractive for the denser Nchain=60 surfaces with more peptoid chains. For example, for the neutral PS, the median energy decreased from -37 kcal mol^{-1} for Nchain=12 to -70 kcal mol^{-1} for Nchain=60 The interaction is also higher for the corresponding charge balanced PSKE brushes (median energies of -50 kcal mol^{-1} and -80 kcal mol^{-1} for Nchain=12 and 60, respectively). This corroborates observations of, e.g., the shorter simulation times needed for the fibronectin domain positions to trend towards the peptoid layers (Fig.2 in main text). Moreover, the increases in the average magnitude of interaction energies going to the denser brush is much less than the factor of five difference in chain densities between the Nchain=12 and 60 surfaces. This further reflects our observation that the Nchain=60 brushes retained an antifouling effect, e.g., the interaction energy does not trend with lower average position of $FnIII_{9-10}$ on the Nchain=60 brush and in fact exhibits high randomness in the interaction energy, with many runs showing lower interaction compared to the Nchain=12 layers (Fig.3 in main text).

The separate (MM and solvation) contributions to the adsorption free energies are given in Table S2. Generally, the MM contribution is favourable and slightly higher in magnitude than the solvation contribution. The solvation contribution is typically unfavourable, reflecting the desolvation of the polar protein and peptoid surfaces during adsorption.

Table S2. Total adsorption free energies and molecular mechanics and solvation contributions (in kcal mol^{-1})

	PS20, Nchain12			PS20, Nchain60			PSKE20, Nchain12			PSKE20, Nchain60		
	ΔG_{ads}	ΔE_{MM}	ΔG_{solv}	ΔG_{ads}	ΔE_{MM}	ΔG_{solv}	ΔG_{ads}	ΔE_{MM}	ΔG_{solv}	ΔG_{ads}	ΔE_{MM}	ΔG_{solv}
1	-82±5	-2260±15	2180±14	-54±2	-815±6	761±6	-34.1±0.7	-755±32	721±31	-51±2	-1747±9	1696±9
2	-31.5±0.5	-324±4	292±4	-52±1	-883±7	831±6	-49.7±0.6	-1348±9	1298±8	-100±3	-1874±13	1774±112
3	-24.6±0.7	202±9	-227±9	-103±3	-1121±7	1018±6	-53.0±0.8	-921±11	868±10	-73±2	-1374±7	1301±7
4	-1.8±0.4	510±5	-511±5	-74±2	-1539±15	1465±15	-69.4±0.7	-1364±5	1294±5	-77±2	-2028±13	1951±13
5	-34.7±0.4	-788±7	753±7	-99±2	-1155±8	1056±8	-71.1±0.6	-1158±6	1087.6	-119±2	-2123±11	2003±11
6	-19±1	750±7	-770±6	-67±2	-816±11	750±11	-70.0±0.7	-1198±5	1128±5	-64±2	-1562±14	1498±14
7	-57.3±0.6	-1315±11	1257±11	-85±2	-1634±8	1549±8	-79.2±0.7	-1861±5	1781±5	-122±3	-1394±19	1271±18
8	-47.3±0.5	-377±7	330±6	-73±2	-1255±11	1182±10	-44.1±0.7	-1169±8	1125±7	-67±2	-1521±25	1454±24
9	-43.2±0.5	-505±4	462±3	-36±2	-56±6	20±6	-10.6±0.4	224±15	-234±15	-83±3	-1336±10	1253±10

1.4. Protein centre-of-mass positions in each simulation run

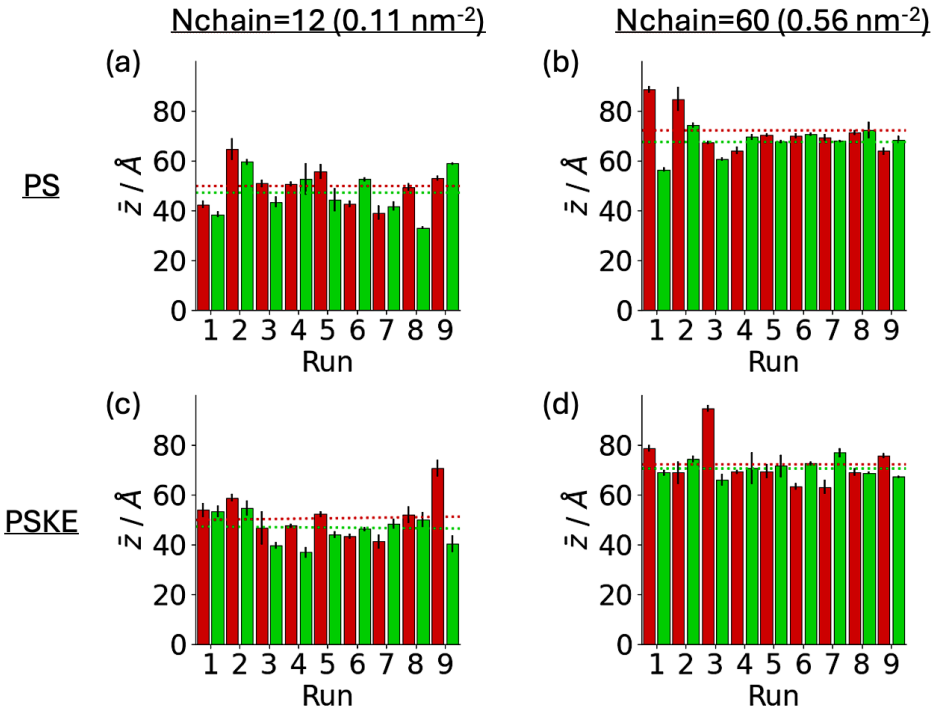

Fig.S4 Average centre-of-mass positions for $FnIII_9$ and $FnIII_{10}$ domains from simulations of $FnIII_{9-10}$ on (a) PS Nchain=12, (b) PS Nchain=60, (c) PSKE Nchain=12, and (d) PSKE Nchain=60. Red and green show centre-of-mass positions for $FnIII_9$ and $FnIII_{10}$ domains, respectively. Dotted lines show average values for each system.

1.5. Average differences in centre-of-mass positions between the full protein and each residue along the sequence in each simulation run

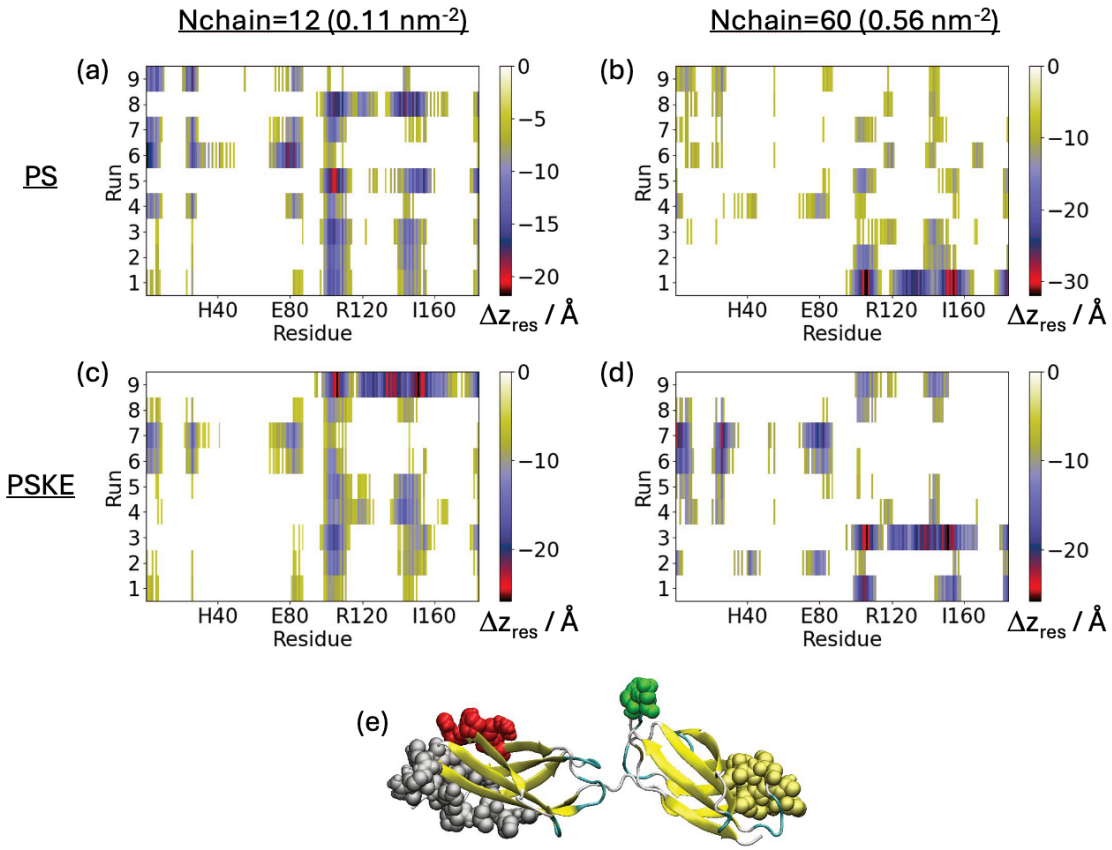

Fig.S5 (a-d) Heat maps showing the average difference in centres-of-mass between each residue and the full FnIII$_{9–10}$ protein for PS Nchain=12 (top left), PS Nchain=60 (top right), PSKE Nchain=12 (bottom left), and PSKE Nchain=60 (bottom right). (e) Example snapshot of FnIII$_{9-10}$ with regions involved in adsorption highlighted in silver (FnIII$_9$) and gold (FnIII$_{10}$), and the synergy and cell binding motifs highlighted in red and green.

1.6. Hydrogen bond assignments to specific residues and amino acid types

Table S3. (a) Residues forming hydrogen bonds with peptoid brush in multiple simulations. Number in parentheses give number of simulation runs where that protein residue forms a hydrogen bond with the peptoid brush. (b) Number of runs categorised by amino acid type. Row colours represent the interaction segment identified in Table 3 in the main text—Purple: linker region (RESIDUES), Yellow: I23-I29 (segment 9a), Pink: N76-G86 (segment 9b), Green: A102-L109 (segment 10a), Blue: T148-G151 (segment 10b); A lighter shade indicates residues adjacent to the primary segments. Residues unrelated to the primary interaction segments are uncoloured.

(a)

	Protein residues
PS, Nchain=12	T6 (2), A24 (2), R78 (2), L83 (3), Q87 (2), E99 (4), T148 (2)
PS, Nchain=60	G1 (2), T6 (2), A24 (2), R26 (4), T104 (3), R120 (2), Y121 (2), T139 (2), K144 (5), T148 (4), R183 (2)
PSKE, Nchain=12	D9 (5), R26 (5), T28 (2), R35 (2), E39 (3), E67 (4), R78 (5), Q87 (3), D97 (2),E99 (5), D113 (3), R120 (3), E128 (2), K144 (3), Y182 (2), R183 (3)
PSKE, Nchain=60	G1 (4), T6 (2), D9 (7), D12 (2), R26 (6), T28 (2), E39 (3), S42 (2), N55 (3), E67 (4), R78 (6), I85 (2), E80 (5), Q87 (3), Q88 (2), E99 (5), T104 (2), S107 (2), W112 (2), D113 (5), T118 (2), R120 (4), S143 (2), K144 (7), S145 (3), T146 (2), T148 (2), S150 (2), D157 (2), R183 (3)

(b)

Peptoid partner	Protein residue	Amino acid													
		K	R	E	D	S	T	Q	N	Y	W	G	A	L	I
PS Nchain=12	T6						2								
	A24												2		
	R78		2												
	L83													3	
	Q87							2							
	E99			4											
	T148						2								
PS Nchain=60	G1											2			
	T6						2								
	A24												2		
	R26		4												
	T104						3								
	R120		2												
	Y121									2					
	T139						2								
	K144	5													
	T148						4								
	R183		2												
PSKE Nchain=12	D9				5										
	R26		5												

	T28						2								
	R35		2												
	E39			3											
	E67			4											
	R78		5												
	Q87							3							
	D97				2										
	E99			5											
	D113				3										
	R120		3												
	E128			2											
	K144	3													
	Y182									2					
	R183		3												
PSKE Nchain=60	G1											4			
	T6						2								
	D9				7										
	D12				2										
	R26		6												
	T28						2								
	E39			3											
	S42					2									
	N55								3						
	E67			4											
	R78		6												
	E80			5											
	I85														2
	Q87							3							
	Q88							2							
	E99			5											
	T104						2								
	S107					2									
	W112										2				
	D113				5										
	T118						2								
	R120		4												
	S143					2									
	K144	7													
	S145					3									
	T146						2								
	T148						2								
	S150					2									
	D157				2										
	R183		3												

1.7. The average number of hydrogen bonds and bridging water molecules for protein-peptoid interactions in each simulation run

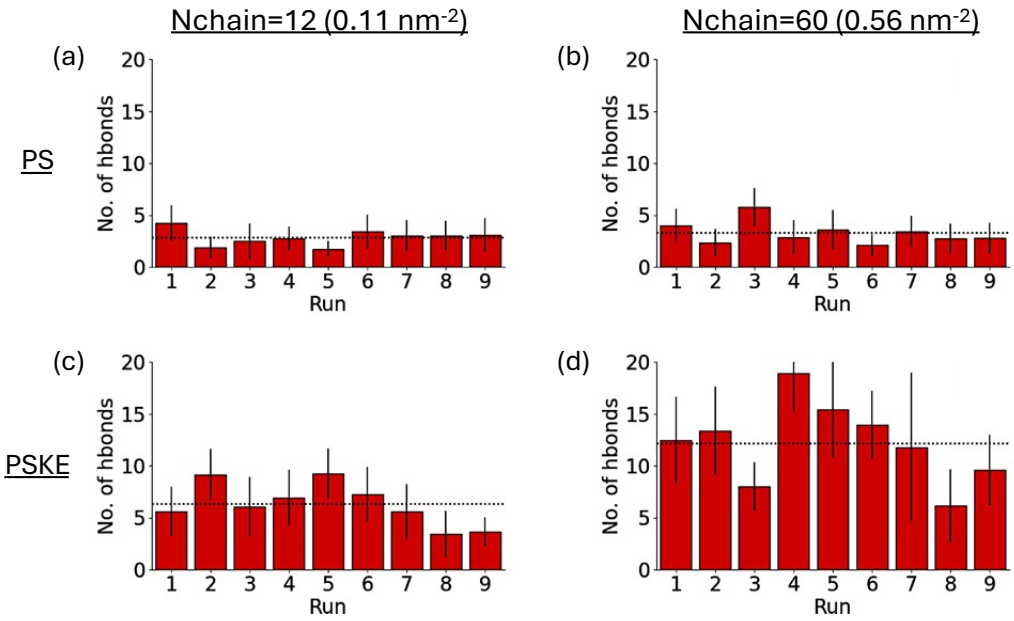

Fig.S6 Average number of protein-peptoid hydrogen bonds for (a) PS, Nchain=12, (b) PS, Nchain=60, (c) PSKE, Nchain=12, and (d) PSKE, Nchain=60 (bottom right).

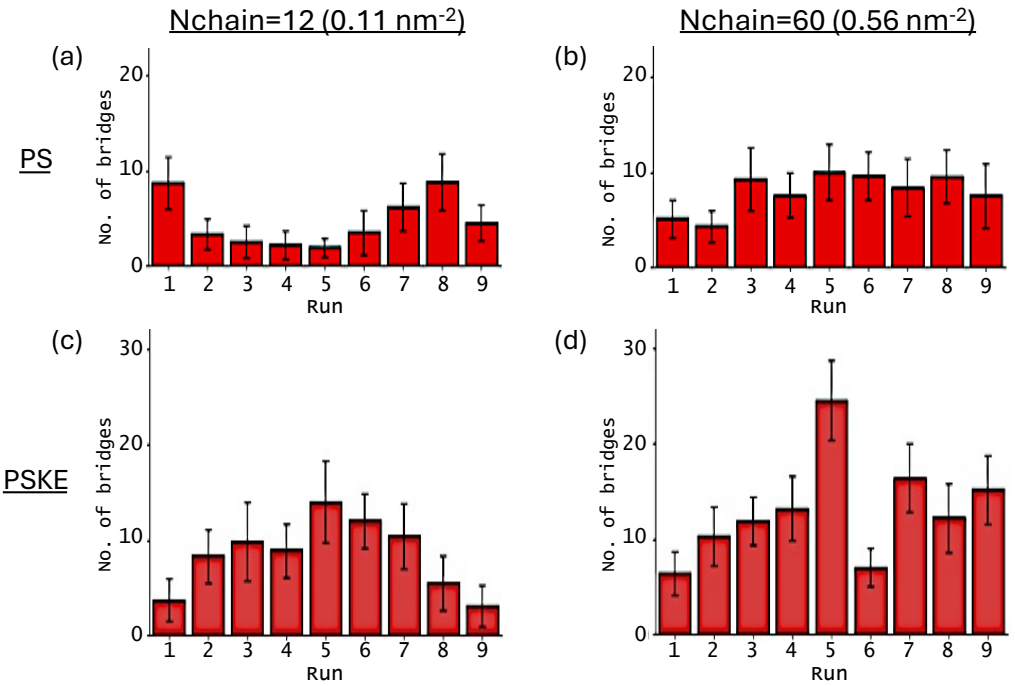

Fig.S7 Average number of bridging water molecules for (a) PS, Nchain=12, (b) PS, Nchain=60, (c) PSKE, Nchain=12, and (d) PSKE, Nchain=60 (bottom right).

1.8. Lateral diffusion coefficients calculated for individual simulation run

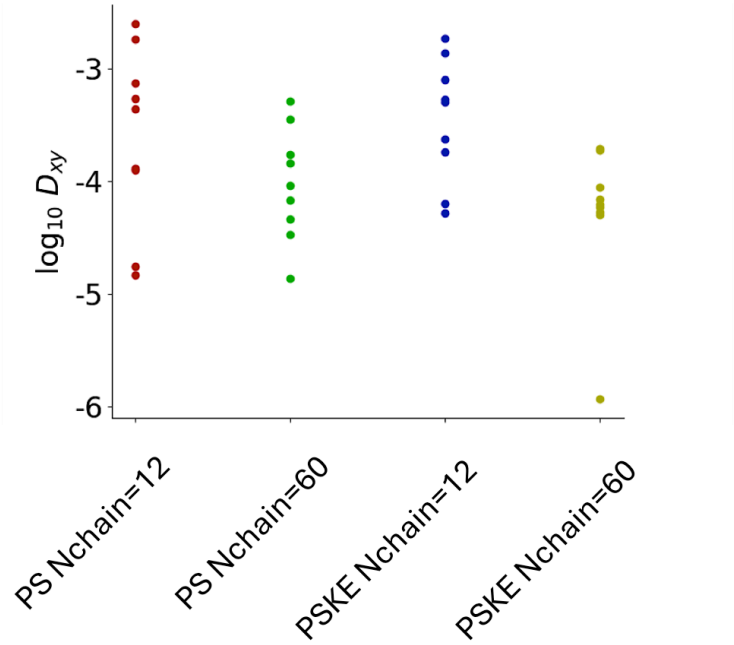

Fig.S8 Lateral diffusion coefficients (in Å^2 ps^{-1}) calculated over last 50 ns of each simulation (see trajectories in Fig.8 in the main text).

1.9. Hydrogen bond autocorrelation functions

The time autocorrelation functions for hydrogen bond formed between the protein and peptoids (h_{ij}) are shown below in Fig.S9. They were calculated as:

$$c(t) = \frac{\langle h_{ij}(t_0) h_{ij}(t_0 + t) \rangle}{\langle h_{ij}(t_0)^2 \rangle}$$

where for each (protein-peptoid) hydrogen bond that is present at time $t = t_0$, $h_{ij}(t_0 + t) = 1$ if a hydrogen bond exists between atoms *i* and *j* at time *t*, and $h_{ij}(t) = 0$ if that hydrogen bond has broken.

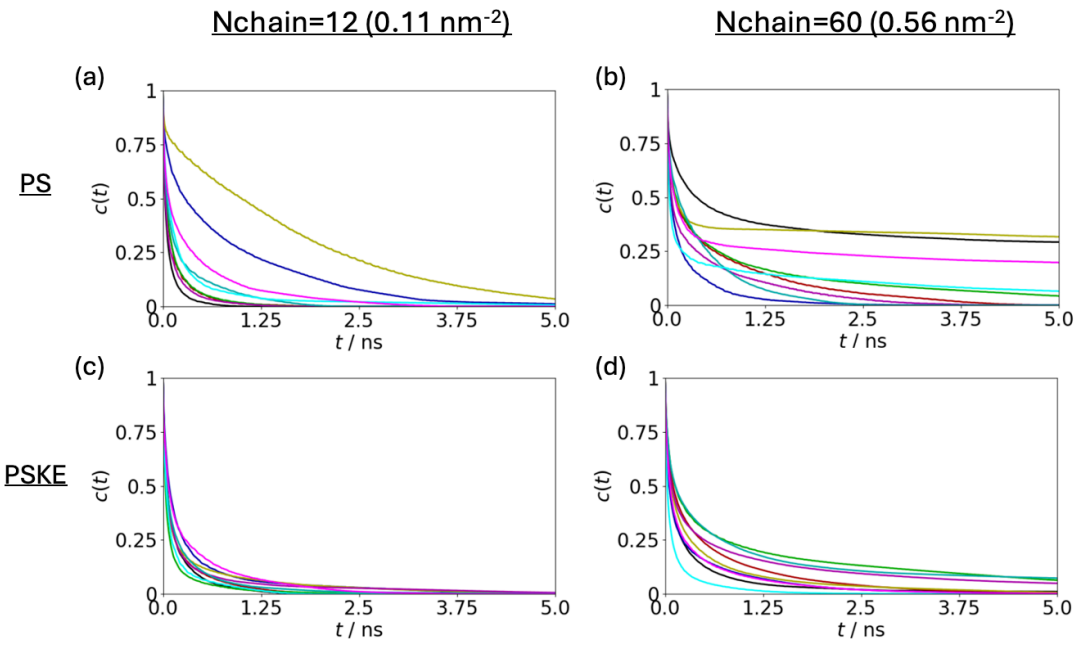

Fig.S9 Protein-peptoid hydrogen bond autocorrelation functions calculated over the last 50 ns of each of the simulations, denoted by different colors. The simulations are for (a) PS, Nchain=12, (b) PS, Nchain=60, (c) PSKE, Nchain=12, and (d) PSKE, Nchain=60 (bottom right).

2. Experimental

PMKE peptoids were sourced from our previous studies, stored at -80^{o}C (ref. 15 in main text). PSKE was synthesized following the solid phase protocol established for the previously published polysarcosine (ref.12 in main text) and PMKE series of peptoids (ref.15 in main text). Briefly, standard submonomer solid phase synthesis was performed using MBHA Rink Amide low loading resin (Novabiochem) and 1M bromoacetic acid (BAA) in DMF and equimolar diisopropylcarbodimide (DIC) for peptoid amide coupling (30 min). The sidechain submonomers used were beta-alanine t-butyl ester-HCl (for Ne) (Sigma-Aldrich) and N-Boc-1,4-butanediamine (for Nk) (Chemimpex, USA) dissolved at 1M in N-methyl-2-pyrrolidone (NMP) (Sigma-Aldrich). Methylamine from commercially available 2 molar THF solutions (Sigma-Aldrich) diluted to 1 M in NMP was used for the polysarcosine residues. Sidechain coupling for sarcosine was 30 min, and those for Ne and Nk were 60 min. Resin cleaving (30-60 min) used standard cleaving cocktail of 95% TFA with 2.5% water and 2.5% triisopropylsilane. Preparative RP-HPLC was used to purify the crude products after diethyl ether precipitation from TFA cleavage. ESI LC-MS and MALDI-MS were used to confirm the mass of the target sequence and verify successful synthesis. Data for the purified PSKE are shown in Figure S7.

The peptoid brush grafting, TiO_2 native oxide film preparation, protein adsorption experiments, and ellipsometry measurements all followed protocols identical to those reported in ref. 12 and 15 in main text). For protein adsorption experiments, lyophilized human fibrinogen (Sigma-Aldrich) was dissolved in pH 7.4, 10 mM hepes buffer, 150 mM NaCl at a nominal concentration of 3 mg/ml. The samples were incubated at 37°C for 20 min and then rinsed in deionized water before ellipsometer measurements. The results are shown in Fig.S1.

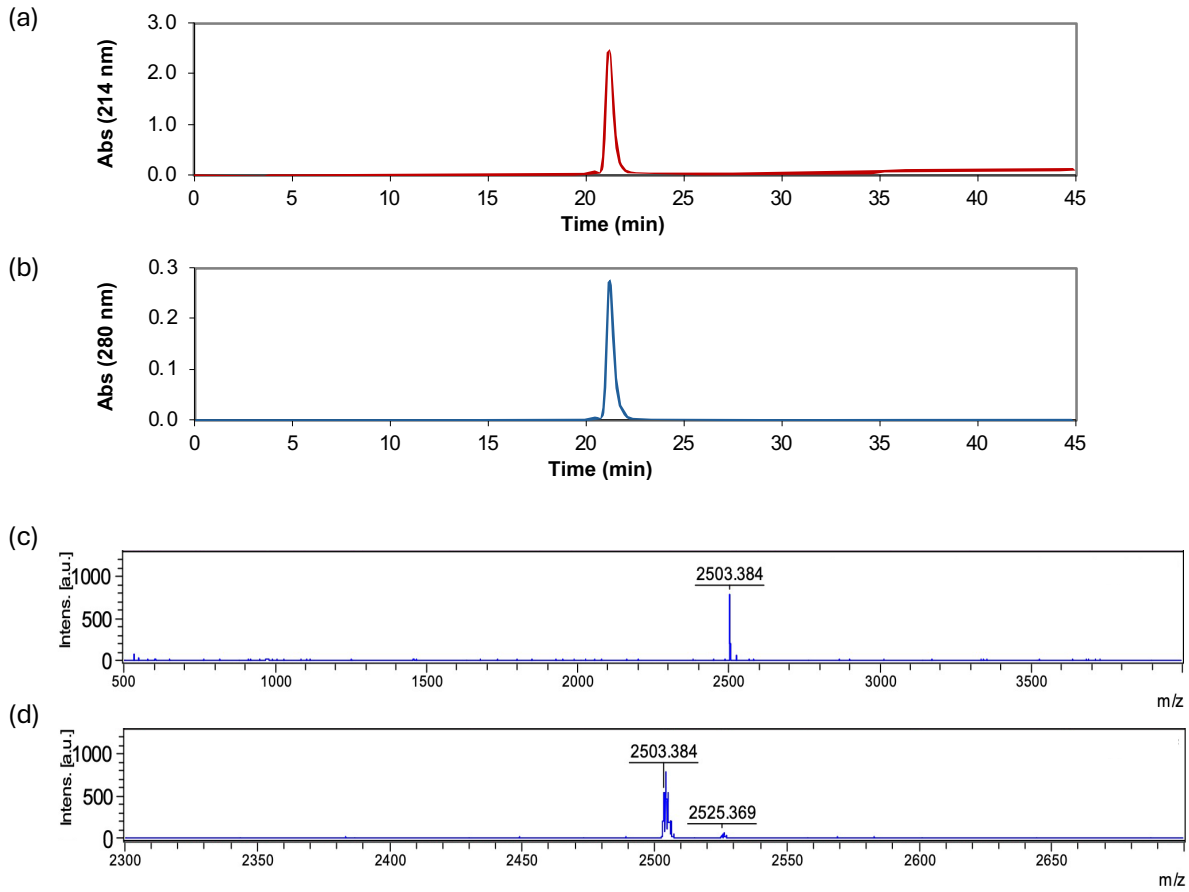

Fig.S10 (a and b) RP-HPLC chromatograms of the purified PSKE peptoid, showing the absorbances with elution time at 214 nm (a) and 280 nm (b). The gradient was 2-30% ACN over 30 min in water using a C18 column (starting after column equilibration from 6 min and ending at 36 min, followed by a 10 min wash at 100% ACN). (c and d) MALDI-MS spectra of the purified PSKE obtained using DHB as the matrix, showing the full spectrum above the matrix peaks (500-4000 m/z) (c) and an expanded view in which the isotopic peaks can be seen (2300-2700 m/z) (d). The expected exact mass of the sequence is 2503.27. The target $[M+H]^+$ was observed at 2503.4, within calibration uncertainty. A sodium adduct $[M+Na]^+$ was also observed at 2525.4 in the expanded view.